Journal of the Mechanics and Physics of Solids 58 (2010) 1397–1410

Contents lists available at ScienceDirect

Journal of the Mechanics and Physics of Solids

journal homepage: www.elsevier.com/locate/jmps

The design of self-collapsed super-strong nanotube bundles

Nicola Maria Pugno [a,b,c,*]

[a] Laboratory of Bio-Inspired Nanomechanics "Giuseppe Maria Pugno", Department of Structural Engineering and Geotechnics, Politecnico di Torino, Corso Duca degli Abruzzi 24, 10129 Torino, Italy
[b] National Institute of Nuclear Physics, National Laboratories of Frascati, Via E. Fermi 40, 00044, Frascati, Italy
[c] National Institute of Metrological Research, Strada delle Cacce 91, I-10135, Torino, Italy

ARTICLE INFO

Article history:
Received 23 December 2009
Received in revised form
23 March 2010
Accepted 16 May 2010

Keywords:
Self-collapse
Nanotube
Bundle
Sliding
Strength

ABSTRACT

The study reported in this paper suggests that the influence of the surrounding nanotubes in a bundle is nearly identical to that of a liquid having surface tension equal to the surface energy of the nanotubes. This surprising behaviour is supported by the calculation of the polygonization and especially of the self-collapse diameters, and related dog-bone configurations, of nanotubes in a bundle, in agreement with atomistic simulations and nanoscale experiments. Accordingly, we have evaluated the strength of the nanotube bundle, with or without collapsed nanotubes, assuming a sliding failure: the self-collapse can increase the strength up to a value of about ~30%, suggesting the design of self-collapsed super-strong nanotube bundles.

Other systems, such as peapods and fullerites, can be similarly treated, including the effect of the presence of a liquid, as reported in the appendices.

© 2010 Elsevier Ltd. All rights reserved.

1. Introduction

An explosion of interest in the scaling-up of buckypapers, nanotube bundles and graphene sheets is taking place in contemporary material science. In particular, nanostructures can be assembled (or well dispersed in a matrix) in order to produce new strong materials and structures. Recently, macroscopic buckypapers (Baughman et al., 1999; Wu et al., 2004; Endo et al., 2005; Wang et al., 2007; Zhang et al., 2005), nanotube bundles (Zhang et al., 2005, 2004; Zhu et al., 2002; Jiang et al., 2002; Dalton et al., 2003; Ericson et al., 2004; Li et al., 2004; Koziol et al., 2007) and graphene sheets (Novoselov et al., 2004; Berger et al., 2006; Stankovich et al., 2006; Dikin et al., 2007) have been realized. In spite of these fascinating achievements of the contemporary material science and chemistry we are evidently far from an optimal result. The reported mechanical strength of buckypapers and graphene sheets, for example, are comparable to that of a classical sheet of paper and macroscopic nanotube bundles have a strength still comparable to that of steel.

In particular, the production of super-strong nanotube bundles remains a challenge of the current material science and could allow the realization of innovative structures, such as a terrestrial space-elevator. Two main failure modes are expected to limit the bundle strength, i.e. (i) nanotube intrinsic fracture or (ii) nanotube sliding. The prevailing mechanism will be that corresponding to the lower strength.

This paper aims to extend the previous calculations performed by the same author, on the strength of nanotubes (Pugno and Ruoff, 2004; Pugno, 2006b, 2006a, 2007) or nanotube bundles (Pugno, 2006, 2007c, 2007b) and assuming the intrinsic fracture of the composing nanotubes (i), for nanotube sliding (ii). For such a case, we have for the first time

* Tel.: +39 11 564 4902; fax: +39 11 564 4899.
E-mail address: nicola.pugno@polito.it

0022-5096/$ - see front matter © 2010 Elsevier Ltd. All rights reserved.
doi:10.1016/j.jmps.2010.05.007

analytically calculated that single walled nanotubes with diameters larger than ~3 nm will self-collapse in the bundle as a consequence of the van der Waals adhesion forces and that the self-collapse can enlarge the cable strength up to ~30%. This suggests the design of self-collapsed super-strong nanotube bundles, corresponding to a maximum cable strength of ~48 GPa, comparable to the thermodynamic limit assuming intrinsic nanotube fracture of km-long cable (see-Pugno, 2007b-, highlighted by *Nature* 450, 6, 2007).

The collapse under pressure, and even under atmospheric pressure, i.e. the self-collapse of nanotubes in bundle, was firstly investigated by atomistic simulations in Elliott et al. (2004). These authors have performed molecular dynamics simulations to confirm that carbon nanotubes undergo a discontinuous collapse transition under hydrostatic pressure, as experimentally observed. These authors also predicted a critical diameter for the self-collapse (at atmospheric pressure), lying between 4.2 and 6.9 nm with the considered force field. In addition, there was good agreement between their simulations, simply calibrated with X-ray compression data for graphite, and the experimentally observed transition pressures for laser-grown nanotubes. This level of agreement raised confidence that the simple and computationally inexpensive force field used in Elliott et al. (2004) may be suitable for examining the nanomechanics of nanotubes. Accordingly, we have compared our theoretical predictions with their atomistic simulations.

Note that the predictions of the nanotube shape after its collapse onto a substrate, induced by adhesion, was treated in-Pugno (2008) with simple nonlinear formulas and found to be in close agreement with atomistic and continuum simulations, suggesting that simple approaches are useful in this context.

Moreover, the self-collapse of nanotubes in a bundle has been recently experimentally observed (Motta et al., 2007). These authors have introduced a method for the direct spinning of pure carbon nanotube fibres from an aerogel formed during chemical vapour deposition. The continuous withdrawal of product from the gas phase as a fibre imparts high commercial potential to the process, including the possibility of in-line post-spin treatments for further product optimisation. Also, they have shown that the mechanical properties of the fibres are directly related to the type of nanotubes present (i.e. multiwall or single wall, diameters, etc.), which in turn, can be, at least ideally, controlled by the careful adjustment of process parameters. In particular, they obtained high performance fibres from dog-bone, i.e. self-collapsed, carbon nanotubes.

In fact, the self-collapse enlarges the interface surface area between the nanotubes and thus also the strength of the junctions between nanotubes and finally the overall fracture strength of the bundle, in case of sliding failure, that is the focus of this paper. The present theory tries to quantify this aspect. Moreover, this work is justified also by the absence of an analytical treatment in the study of the self-collapse of nanotubes in a bundle, and we hope it will be of a general interest for the design of super-strong nanotube bundles of the next generation.

2. On the polygonization, collapse, self-collapse and "dog-bone" configurations of an isolated nanotube or of nanotubes in a bundle

2.1. Polygonization

Due to surface energy (mainly van der Waals attraction) and/or external pressure the nanotubes in a bundle tend to polygonize (e.g. see Elliott et al., 2004), from the circular towards the hexagonal shape, Fig. 1a.

In general, a blunt hexagon is expected for a nanotube with a small number of walls, e.g. single, double or triple walled nanotubes. Let us indicate the radius of the blunt notches with r and the length of the rectilinear sides with a. Denoting with R the nanotube radius, the inextensibility condition implies $2\pi R=6a+2\pi r$, from which we deduce

$$r(a)=R-\frac{3}{\pi}a \tag{1}$$

The nanotube cross-sectional area is

$$A(a)=6ar+\pi r^2+\frac{3}{2}\sqrt{3}a^2=6a\left(R-\frac{3}{\pi}a\right)+\pi\left(R-\frac{3}{\pi}a\right)^2+\frac{3}{2}\sqrt{3}a^2 \tag{2}$$

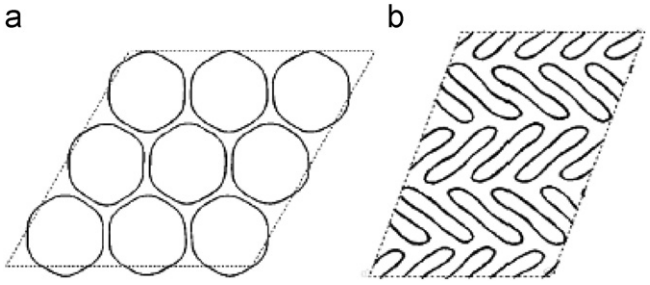

Fig. 1. (a) Polygonization of nanotubes in a bundle, calculated according to atomistic simulations. (b) Collapse of nanotubes in a bundle, calculated according to atomistic simulations (Elliott, J.A., Sandler, J.K., Windle, A.H., Young, R.J., Shaffer, M.S., 2004. Collapse of single-wall carbon nanotubes is diameter dependent. Physical Review Letters 92, 095501. Copyright (2004) by The American Physical Society.)

and consequently $a(A)=\sqrt{(\pi R^2-A)/(c/2)}$, with $c=18/\pi-3\sqrt{3}\approx 0.54$. Posing $A_0=\pi R^2$ and $\Delta A=A_0-A$, we can introduce $0\le a^*\equiv a/R\le \pi/3$:

$$a^*=\frac{a}{R}=\sqrt{\frac{2\pi}{c}}\sqrt{\frac{\Delta A}{A_0}} \tag{3}$$

Note that a^* is proportional to the relative contact length as well as to the relative area/volume variation.

The equilibrium of the system can be calculated by minimizing its free energy. Indicating with Φ the elastic energy, with γ the surface energy and with p the external (relative) pressure, the energy minimization implies

$$\mathrm{d}\Phi+pL\,\mathrm{d}A-6\gamma L\,\mathrm{d}a=0 \tag{4}$$

where L is the nanotube length.

According to elasticity, the strain energy stored per unit surface is $\frac{\mathrm{d}\Phi}{Lr\mathrm{d}\vartheta}=\frac{N^\alpha D}{2r^2}$ (ϑ is the angle describing the surface at the radius r), where

$$D=\frac{Et^3}{12(1-\nu^2)} \tag{5}$$

is the nanotube (shell) bending rigidity, N is the number of walls and $1\le\alpha\le 3$: assuming perfect bonding between the walls would correspond to $\alpha=3$, whereas for independent walls $\alpha=1$ (however note that in the equations appears always the group $N^\alpha D$, that is the total bending stiffness); E is the Young's modulus of graphene and $t\approx 0.34$ nm is the conventional wall thickness.

Accordingly, $\Phi=\frac{\pi DL}{r}$ and $\frac{\mathrm{d}\Phi}{\mathrm{d}a}=\frac{3N^\alpha DL}{r^2}$. In addition, $\frac{\mathrm{d}A}{\mathrm{d}a}=-ca$. Thus, the free energy minimization yields

$$p(a^*)=\frac{3N^\alpha D}{ca^*(1-(3/\pi)a^*)^2R^3}-\frac{6\gamma}{ca^*R} \tag{6}$$

Under zero pressure the equilibrium is reached in the following configuration:

$$a_0^*=a^*(p=0)=\frac{\pi}{3}\left(1-\frac{1}{R}\sqrt{\frac{N^\alpha D}{2\gamma}}\right) \tag{7}$$

showing that for radii

$$R\le R_0^{(N)}=\sqrt{\frac{N^\alpha D}{2\gamma}} \tag{8}$$

the contact length is physically zero (mathematically it is negative) and thus the surface energy is not capable of producing even an infinitesimal polygonization in very small nanotubes. This peculiarity, of zero contact length for small radii, is also observed during the adhesion of single walled nanotubes over a flat substrate (Pugno, 2008). Taking $D=0.11$ nN nm (bending stiffness of graphene $D\approx 0.09$–0.24 nN nm, see Pugno 2008), thus D is not calculated here using the continuum approximation of Eq. (5)) and $\gamma=0.18$ N/m (surface energy of graphene $\gamma\approx 0.16-0.20$ N/m, see Pugno, 2008), we find $2R_0^{(1)}\approx 1.1$ nm. Assuming an intermediate coupling between the walls, i.e. $\alpha\approx 2$, the critical diameters for double and triple walled nanotubes are $2R_0^{(2)}\approx 2.2$ and $2R_0^{(3)}\approx 3.3$ nm. The intermediate value of $\alpha\approx 2$ is more plausible than its limiting cases and, as we will see in the following, it is in closer agreement with a large number of different observations. However, we are conducting *ad hoc* atomistic simulations, to be extensively compared with our theory and to be presented in subsequent papers.

For larger nanotubes, the adhesion energy induces a polygonization, as described by Eq. (7). The action of an external pressure further increases the polygonization, according to the state Eq. (6), see Fig. 2.

Note that Eqs. (1) and (7) imply that under zero pressure the blunt radius r assumes the constant value $R_0^{(N)}$, as defined in Eq. (8).

2.2. Collapse

Eq. (6) correctly predicts that to reach a full polygonization the pressure must tend to infinity, as the elastic energy stored in sharp notches, namely $p\to\infty$ for $a_0^*\to\pi/3$; practically, a different mechanism, that is the well-known elastic instability, Fig. 1b, will take place at a finite value of the applied pressure.

We treat the large nanotube bundle as a liquid-like material (for the additional presence of a liquid see Appendix A) with surface tension $\gamma_t=\gamma$, as imposed by the energy equivalence (the surface tension has the thermodynamic significance of work spent to create the unit surface, as the surface energy), thus deducing a pressure γ/R acting on a single nanotube of radius R within a bundle, as evinced by Laplace's equation. In other words, considering a cylindrical cavity/nanotube of size R under a pressure p in a liquid/nanotube bundle having surface tension/energy γ, the free energy (per unit length) of the system can be written as $E=-p(\pi R^2)+\gamma(2\pi R)+const$ and has to be minimal at the equilibrium; thus posing $\mathrm{d}E=0$, we find $p=\gamma/R$. Note that for a crystal composed by fullerenes (see Appendix B, where also mixed systems, e.g. peapods, are treated)

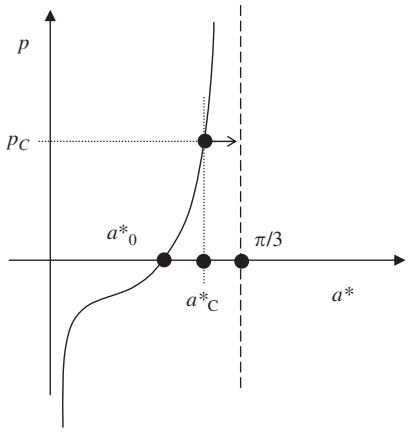

Fig. 2. State Eq. (6) for the polygonization of nanotubes in a bundle. (An inflection point appears at a negative pressure, but the curve has everywhere a positive slope, thus the process is stable.)

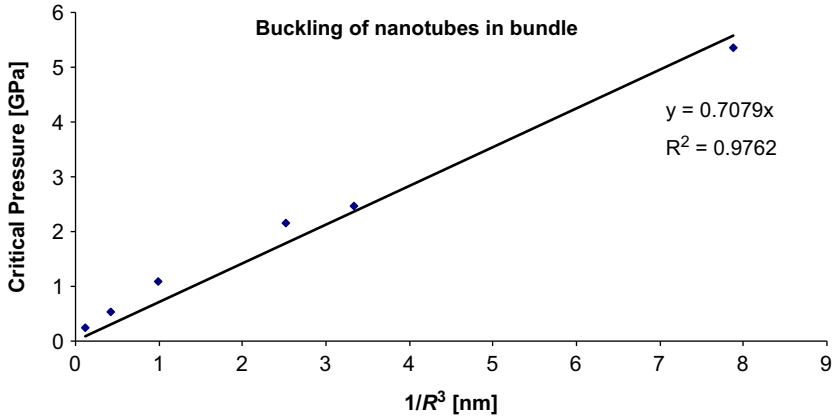

Fig. 3. Collapse of nanotubes in a bundle, comparison between theory (line) and atomistic simulations (Elliott et al., 2004) (dots); total critical pressure $p_C+\gamma/R$ versus $1/R^3$, the slope is thus $3D$.

of radius R, the pressure $p=2\gamma/R$ on a fullerene could be deduced from $E=-p((4/3)\pi R^3)+\gamma(4\pi R^2)+const$ posing $dE=0$, again in agreement with the prediction of Laplace's equation.

The critical pressure can be accordingly derived as

$$p_C=\frac{3N^{\alpha}D}{R^3}-\frac{\gamma}{R} \tag{9}$$

The first term in Eq. (9), for $\alpha=3$, is that governing the buckling of a perfectly elastic cylindrical long thin shell (of thickness Nt), whereas the second term is the pressure imposed by the surrounding nanotubes.

Treating the atomistic simulations results for single walled nanotubes (Elliott et al., 2004), excluding the two smallest nanotubes for which the buckling pressure was not accurately determined, a relevant agreement with Eq. (9) is observed (coefficient of correlation $R^2=0.98$), fitting a plausible value of $D_{fit}\approx 0.2$ nN nm, see Fig. 3.

2.3. Self-collapse

From Eq. (9) we derive the following condition for the self-collapse, i.e. collapse under zero pressure, of a nanotube in a bundle:

$$R\geq R_C^{(N)}=\sqrt{\frac{3N^{\alpha}D}{\gamma}}=\sqrt{6}R_0^{(N)} \tag{10}$$

In the presence of internal vacuum and external atmospheric pressure, the self-collapse pressure must be considered not zero but the atmospheric pressure $p_A\approx 0.1$ MPa. However this value is small and does not significantly affect the prediction of Eq. (10). In fact, new self-collapse radius can be calculated according to Eq. (9) with $p_C=p_A$, solving the corresponding third-order polynomial equation. However, a correction with respect to the previously evaluated

self-collapse radius $R_C^{(N)}$ can be considered inserting into Eq. (10) $R \to R(1+\varepsilon)$, neglecting the powers of ε higher than one and noting that $R_C^{(N)}$ is the solution of the equation for $p_C=0$; we accordingly find $\varepsilon = -ca_C^* R_C^{(N)} p_A/(6\gamma)$; this number is of the order of $\varepsilon \approx -R_C^{(N)} p_A/\gamma \approx -10^{-4}$ and confirms the hypothesis.

Taking $D=0.11$ nN nm and $\gamma=0.18$ N/m we find $2R_C^{(1)} \approx 2.7$ nm. Considering an intermediate coupling between the walls ($\alpha \approx 2$), the critical diameters for double and triple walled nanotubes are $2R_C^{(2)} \approx 5.4$ and $2R_C^{(3)} \approx 8.1$ nm.

In Motta et al. (2007), 17 experimental observations on the self-collapse of nanotubes in a bundle have been reported, see Fig. 4 and related Table 1. A number of 5 single walled nanotubes with diameters in the range 4.6–5.7 nm were all observed as collapsed; moreover, while the 3 double walled nanotubes observed with internal diameters in the range 4.2–4.7 nm (the effective diameters are larger by a factor of $\sim$0.34/2 nm) had not collapsed, the observed 8 double walled nanotubes with internal diameters in the range 6.2–8.4 nm had collapsed. Finally, a triple walled nanotube of 14 nm internal diameter (the effective diameter is $\sim$14.34 m) was observed as collapsed too. All these 17 observations are in agreement with our theoretical predictions of Eq. (10), supporting our conjecture of liquid-like nanotube bundles.

2.4. "Dog-bone" configuration

The collapsed nanotubes assume a characteristic "dog-bone" cross-sectional shape, since the radius of curvature cannot be infinitely small, see Figs. 4 and 5.

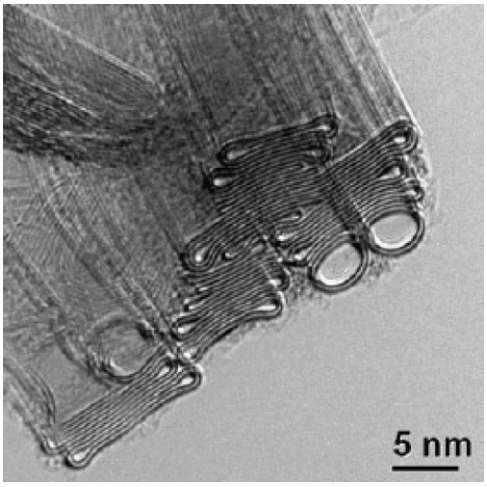

Fig. 4. Self-collapsed nanotubes in a bundle (Motta, M.S., Moisala, A., Kinloch, I.A., Windle, A.H., 2007. High performance fibres from 'Dog Bone' carbon nanotubes. Advanced Materials 19, 3721–3726. Copyright Wiley-VCH Verlag GmbH & Co. KGaA. Reproduced with permission.).

Table 1
Self-collapse of nanotubes in a bundle: our theory exactly fits the experimental observations (Motta et al., 2007).

Nanotube number	Number N of walls	Diameter of the internal wall (nm)	Collapsed (Y/N) Exp. and Theo.
1	1	4.6	Y
2	1	4.7	Y
3	1	4.8	Y
4	1	5.2	Y
5	1	5.7	Y
6	2	4.2	N
7	2	4.6	N
8	2	4.7	N
9	2	6.2	Y
10	2	6.5	Y
11	2	6.8	Y
12	2	6.8	Y
13	2	7.9	Y
14	2	8.3	Y
15	2	8.3	Y
16	2	8.4	Y
17	3	14.0	Y

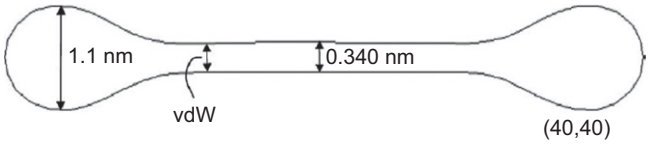

Fig. 5. "Dog-bone" configuration, calculated according to finite element simulations (Pantano, A., Parks, D.M., Boyce, M.C., 2004. Mechanics of deformation of single- and multi-wall carbon nanotubes. Journal of the Mechanics and Physics of Solids 52, 789–821. Copyright (2004), with permission from Elsevier.).

In order to derive the equilibrium of the dog-bone configuration, the free energy minimization can again be considered. Let us indicate with r the radius of the two terminal lobes and with a the length of the two rectilinear sides in mutual contact. Denoting with R the nanotube radius, the inextensibility condition implies $2\pi R=2a+4\pi r$, from which we deduce

$$r=\frac{R}{2}-a/(2\pi) \tag{11}$$

The nanotube cross-sectional area is

$$A=2\pi r^2 \tag{12}$$

The energy minimization implies $\left(\Phi=\frac{2\pi N^{\alpha}DL}{r}\right)$

$$\frac{d\Phi}{dr}+pL\frac{dA}{dr}-2\gamma L\frac{da}{dr}=0 \tag{13}$$

corresponding to the following equilibrium:

$$p(r)=\frac{N^{\alpha}D}{2r^3}-\frac{\gamma}{r} \tag{14}$$

For zero surface energy the equilibrium pressure is positive (inward), whereas complementary for zero bending stiffness it is negative (outward). Under zero pressure the equilibrium is reached for

$$r_0=\sqrt{\frac{N^{\alpha}D}{2\gamma}}=R_0^{(N)} \tag{15}$$

In such a case, we predict an equilibrium diameter for a single walled nanotube of $2r_0\approx 1.1$ nm, in perfect agreement with previous calculations (see Fig. 5).

Posing $a=0$ in Eq. (11) and comparing with Eq. (14), we deduce the critical pressure corresponding to the dog-bone "opening" (since the process is stable, see in the following):

$$p_O=\frac{4N^{\alpha}D}{R^3}-\frac{2\gamma}{R} \tag{16}$$

Moreover, posing $p_O=0$ in Eq. (16) suggests that for nanotube radii

$$R\le\sqrt{\frac{2N^{\alpha}D}{\gamma}}=2R_0^{(N)} \tag{17}$$

the "dog-bone" configuration cannot be self-maintained (for single nanotubes such a diameter is $2R_O\approx 2.2$ nm).

Note that Eq. (14) presents an inflection point with zero slope at $r=\sqrt{3}r_0$, suggesting that at such a point a rapid change in the configuration will take place at an "anti-buckling" pressure

$$p(r=\sqrt{3}r_0)=-\frac{2\gamma}{3\sqrt{3}r_0}=-\frac{4}{3\sqrt{6N^{\alpha}}}\sqrt{\frac{\gamma^3}{D}}$$

If the nanotube is assumed to be in contact with other adjacent nanotubes along its two external sides of length a, the equations presented in this section are still valid with the substitution $\gamma\to 2\gamma$.

3. Calculation of the strength and toughness of nanotube bundles under sliding failure

3.1. Strength

The fracture mechanics approach developed by this author in several papers (e.g. see for instance Pugno, 1999; Pugno and Carpinteri, 2003) could be of interest to evaluate the strength of nanotube bundles assuming a sliding failure mode (Pugno, 2007a). This hypothesis is complementary to that of intrinsic nanotube fracture, already treated by the same author in numerous papers (e.g. see for instance, Pugno, 2006, 2007c, 2007b) in the context of the space-elevator. Thus we assume the interactions between adjacent nanotubes as the weakest-links, i.e. that the fracture of the bundle is caused by nanotube sliding rather than by the intrinsic nanotube fracture.

Accordingly, the energy balance during a longitudinal delamination (here "delamination" has the meaning of Mode II crack propagation at the interface between adjacent nanotubes) dz under the applied force F, is

$$d\Phi - F\,du - 2\gamma(P_C + P_{vdW})dz = 0 \tag{18}$$

where dΦ and du are the strain energy and elastic displacement variation due to the infinitesimal increment in the compliance caused by the delamination dz; P_{vdw} describes the still existing van der Waals attraction (e.g. attractive part of the Lennard–Jones potential) for vanishing nominal contact nanotube perimeter $P_C=6a$ (the shear force between two graphite single layers becomes zero for nominally negative contact area); $6a$ is the contact length due to polygonization of nanotubes in the bundle, caused by their surface energy γ. Elasticity poses $d\Phi/dz = -F^2/(2ES)$, where S is the cross-sectional surface area of the nanotube, whereas according to Clapeyron's theorem $F\,du=2\,d\Phi$. Thus, the following simple expression for the bundle strength ($\sigma_C=F_C/S$, effective stress and cross-sectional surface area are here considered; F_C is the force at fracture) is predicted:

$$\sigma_C^{(theo)} = 2\sqrt{E\gamma\frac{P}{S}} \tag{19}$$

in which it appears the ratio between the effective perimeter ($P=P_C+P_{vdW}$) in contact and the cross-sectional surface area of the nanotubes.

Eq. (19) can be considered valid also for the entire bundle, since we are assuming here the same value P/S for all the nanotubes in the bundle; the fact that the strength is not a function of the nanotube numbers or bundle diameter is for this same reason, i.e. because we are not assuming here a "defect" size distribution for S/P – that basically represents a characteristic defect size – but a constant value for all the nanotubes in the bundle; of course, assuming a statistical distribution for the characteristic defect size S/P with the upper limit proportional to the structural size (the larger the structure, the larger is the largest defect) would imply a size-effect, thus a dependence on the nanotube numbers or bundle diameter. Nevertheless here we are interested in the simplest model (i) and in the upperbound strength predictions (ii), thus we do not consider statistics into Eq. (19).

Note that Eq. (19) is basically the asymptotic limit for sufficiently long overlapping length, that is the length along with two adjacent nanotubes are nominally in contact, for overlapping length smaller than a critical value the strength increases by increasing the overlapping length, see-Pugno (2007a), for a single nanotube this overlapping length is of the order of 10 μm, whereas it is expected to be larger for nanotubes in bundles, e.g. of the order of several millimetres, as confirmed experimentally. This critical length is (Pugno, 1999)

$$\ell_C \approx 6\sqrt{\frac{hES}{PG}} \tag{20}$$

where h and G are the thickness and shear modulus of the interface. Eq. (20) suggests that increasing the size-scale $L\propto\sqrt{S}\propto P\propto h$ this critical length increases too, namely $\ell\propto L$, thus the strength increases by increasing the overlapping length in a wider range; however note that the achievable strength is reduced since, $\sigma_C^{(theo)}\propto\sqrt{h}\ell^{-1}\propto\sqrt{P/S}\propto L^{-1/2}$ if $L\propto\ell\propto h$: increasing the overlapping length ad infinitum is not a way to indefinitely increase the strength.

The real strength could be significantly smaller, than that predicted by Eq. (20), not only because $\ell<\ell_C$ but also as a consequence of the misalignment of the nanotubes with respect to the bundle axis. Assuming a non perfect alignment of the nanotubes in the bundle, described by a nonzero angle β (here assumed identical for all the nanotubes in the bundle, even if – also in this case, as for the characteristic defect size S/P – a proper statistics could be invoked for this parameter), the longitudinal force carried by the nanotubes will be $F/\cos\beta$, thus the equivalent Young's modulus of the bundle will be $E\cos^2\beta$, as can be evinced by the corresponding modification of the energy balance during delamination; accordingly,

$$\sigma_C = 2\cos\beta\sqrt{E\gamma\frac{P}{S}} \tag{21}$$

The maximal achievable strength is predicted for collapsed perfectly aligned (sufficiently overlapped) nanotubes, i.e. $P/S\approx 1/(Nt)$, $\beta=0$:

$$\sigma_C^{(theo,N)} = 2\sqrt{\frac{E\gamma}{Nt}} \tag{22}$$

Taking $E=1$ TPa (Young's modulus of graphene), $\gamma=0.2$ N/m (surface energy of graphene; however note that in reality γ could be also larger as a consequence of additional dissipative mechanisms, e.g. fracture and friction in addition to adhesion), the predicted maximum strength for single walled nanotubes ($N=1$) is

$$\sigma_C^{(max)} = \sigma_C^{(theo,1)} = 48.5\,\text{GPa} \tag{23}$$

whereas for double or triple walled nanotubes $\sigma_C^{(theo,2)}=34.3$ or $\sigma_C^{(theo,3)}=28.0$ GPa.

Considering the previous calculations for the equilibrium contact length a during polygonization, we can write

$$\sigma_C = 2\cos\beta\sqrt{E\gamma\frac{6a+P_{vdW}}{S}} \tag{24}$$

3.2. Strength increment caused by the self-collapse

According to the previous analysis, the ratio between the bundle strength $\sigma_C^{(0)}$, in the presence of self-collapse, and $\sigma_C^{(O)}$, in the absence of self-collapse, is predicted to be

$$\frac{\sigma_C^{(0)}}{\sigma_C^{(O)}}=\sqrt{\frac{2\pi R+P_{vdW}}{2\pi R\left(1-\frac{1}{R}\sqrt{\frac{N^{\alpha}D}{2\gamma}}\right)+P_{vdW}}} \quad \text{for } R\geq R_C^{(N)}=\sqrt{\frac{3N^{\alpha}D}{\gamma}} \tag{25}$$

The maximal strength increment induced by the self-collapse is thus

$$\left.\frac{\sigma_C^{(0)}}{\sigma_C^{(O)}}\right|_{\max}=\sqrt{\frac{1}{1-1/\sqrt{6}}}\approx 1.30 \tag{26}$$

Eq. (26) shows that the self-collapse could enhance the nanotube bundle strength up to ~30%. The reason is obviously the incremented surface area of the interfaces between the nanotubes.

3.3. Toughness

The energy dissipated during the fracture of the bundle is

$$W_C\approx F_C\ell \tag{27}$$

where ℓ is the mean nanotube length and (before separation a sliding of length $\sim\ell$ occurs at a constant force $\sim F_C$, (Pugno, 1999). Accordingly, the effective fracture energy per unit area of the bundle is

$$G_C\approx\sigma_C\ell \tag{28}$$

Taking σ_C=10 GPa and ℓ=1 μm gives $G_C\approx 10^4$ N/m, corresponding to a facture toughness of

$$K_C=\sqrt{G_C E} \tag{29}$$

of the order of $K_C\approx 100\,\text{MPa}\sqrt{\text{m}}$ (E=1 TPa). The energy per unit area is high but not proportional to the bundle length, thus suggesting a quasi-brittle, rather than ductile, behaviour. Eq. (28) suggests to increase the nanotube length, in order to increase the toughness; in the limit of coincident nanotube and bundle lengths (still assuming the sliding failure, practically a composite bundle would be more appropriate in order to diffuse the damage in the entire bundle volume prior to fracture), the dissipated energy reached at a failure strain of $\varepsilon_C\approx 100\%$, per unit volume or mass, becomes

$$J_{CV}^{(max)}\approx\sigma_C,\quad J_{CM}^{(max)}\approx\frac{\sigma_C}{\rho} \tag{30}$$

where ρ is the material density. Taking σ_C=10 GPa and $\rho\approx 1000\,\text{kg/m}^3$ yields a maximum dissipated energy per unit mass of ~10 MJ/g, enormously higher than that of spider silk (~165 J/g). Even if the predictions of Eq. (30) are fully ideal, and thus not realistic as a consequence of an expected failure localization, they suggest that we are far from such a limit for toughness and thus that super-tough composites can be produced in the near future (much more easily than super-strong composites: there is plenty of room at the bottom for toughness, more than for strength).

3.4. Hierarchical bundle

Experimentally, three hierarchies of structure within the fibre can be observed (Motta et al., 2007): doubly walled nanotubes with diameters in the range 5–10 nm, bundles of 20–60 nm diameter composed by self-collapsed nanotubes and, finally, the macroscopic fibre composed by bundles with preferred orientation along the fibre axis, see Fig. 6.

In such a case Eq. (24) is still valid, but the proper value of the ratio P/S must be evaluated, according to the hierarchical nature of the fibre. Consider two sub-bundles, having surface energy γ, Young's modulus E, Poisson's ratio ν and radius R; the well-known JKR theory of adhesion gives the contact width as (see Pugno et al., 2008)

$$w=4\left(\frac{4R^2\gamma(1-\nu^2)}{\pi E}\right)^{1/3} \tag{31}$$

Assuming a hexagonal packing of the bundles within the fibre and independent contact widths, we deduce

$$\frac{P}{S}=\frac{24\left(\frac{4R^2\gamma(1-\nu^2)}{\pi E}\right)^{1/3}}{\pi R^2} \tag{32}$$

Finally, the strength for the bundle is predicted according to

$$\sigma_C=2\cos\beta\sqrt{E\gamma\frac{P}{S}}=2\cos\beta\sqrt{E\gamma\frac{24\left(\frac{4R^2\gamma(1-\nu^2)}{\pi E}\right)^{1/3}}{\pi R^2}}$$

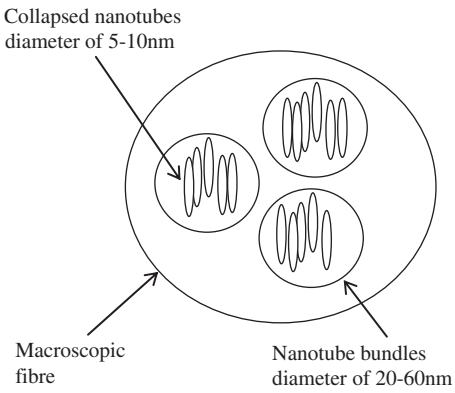

Fig. 6. Scheme of the cross-section of the hierarchical nanotube fibre, according to experimental observations (Motta et al., 2007).

$$=\frac{2\sqrt{24}(4(1-\nu^2))^{1/6}}{\pi^{2/3}}\cos\beta E^{1/3}\gamma^{2/3}R^{-2/3}\approx 5.76\cos\beta E^{1/3}\gamma^{2/3}R^{-2/3} \tag{33}$$

Taking $E=1$ TPa, $\nu=\beta=0$, $\gamma=0.2$ N/m, $R=10$–30 nm, we deduce $(S/P)\approx 112$ nm and thus $\sigma_C^{(theo)}\approx 2.04-4.24$ GPa. These values are in close agreement to the experimental observations (Motta et al., 2007), even if we have taken for E, ν, β, γ just plausible values rather than independently measured or fitting values.

The analysis suggests to reduce the sub-bundles radius in order to increase the strength, as well as to increase the nanotube length to enlarge the toughness, but only up to ℓ_C in order not to be detrimental for the strength (see also Pugno, 2006c).

4. Conclusions

We have presented a new theory for designing super strong nanotube bundles, with enhanced strength, thanks to the activation of the self-collapse of the composing nanotubes. The self-collapse of a nanotube is due to its elastic buckling induced by the internal pressure generated by the surrounding nanotubes as a consequence of the surface energy of the bundle, similarly to what can be observed in a liquid with a given surface tension. The self-collapse enlarges the interface surface area between the nanotubes, and thus the strength of the nanotube junctions and ultimately the bundle strength. Hierarchical bundles are also considered. All the theoretical predictions are in good agreements with related nanoscale experiments and atomistic simulations.

The model supports the idea that the influence of the surrounding nanotubes in a bundle is similar to that of a liquid having surface tension equal to the surface energy of the nanotubes. This surprising behaviour is confirmed by the calculation of the self-collapse diameters of nanotubes in a bundle, as well as by dog-bone and polygonized configurations. We have for the first time analytically calculated that single walled nanotubes with diameters larger than ~ 3 nm will self-collapse in the bundle as a consequence of the van der Waals adhesion forces and that the self-collapse can enlarge the cable strength up to $\sim 30\%$. This suggests the design of self-collapsed super-strong nanotube bundles, corresponding to a maximum cable strength of ~ 48 GPa, comparable to the thermodynamic limit assuming intrinsic nanotube fracture of a km-long cable. Other systems, such as peapods and fullerites, can be similarly treated, including the effect of the presence of a liquid (Pugno, 2009), as reported in Appendices A and B.

Appendix A. The role of a liquid phase on the polygonization, collapse, self-collapse and "dog-bone" configurations of an isolated nanotube or of nanotubes in a bundle

A.1. Polygonization

A liquid phase around a bundle of radius R_B induces an additional pressure γ_t/R_B, according to Laplace's equation, where γ_t is the liquid surface tension. Accordingly, the equation of state for the polygonization becomes

$$p(a^*)=\frac{3N^\alpha D}{ca^*(1-(3/\pi)a^*)^2R^3}-\frac{\gamma_t}{R_B}-\frac{6\gamma_{wet}}{ca^*R} \tag{34}$$

where γ_{wet} is the surface energy of the nanotubes in the presence of the liquid.

Without liquid and external pressure ($\gamma_t=p=0$, $\gamma_{wet}\to\gamma_{dry}$) the equilibrium is reached in the following configuration:

$$a^*_{0dry}=a^*(p=\gamma_t=0)=\frac{\pi}{3}\left(1-\frac{1}{R}\sqrt{\frac{N^\alpha D}{2\gamma_{dry}}}\right) \tag{35}$$

In the presence of liquid and without an additional external pressure, the new equilibrium contact length can be calculated according to Eq. (34) posing $p=0$ and solving the corresponding third-order polynomial equation. However, a correction with respect to a^*_{0dry} can be deduced inserting into Eq. (34) $a^*=a^*_{0dry}(\gamma_{dry}\to\gamma_{wet})(1+\varepsilon_a)$, neglecting the powers of $\varepsilon_a\ll 1$ higher than one and recalling Eq. (35); we accordingly find

$$\varepsilon_a=\frac{\pi c\gamma_t}{36R_B\gamma_{wet}}\sqrt{\frac{N^\alpha D}{2\gamma_{wet}}} \tag{36}$$

Thus, the equilibrium configuration in the presence of liquid is

$$a^*_{0wet}=a^*(p=0)\approx\frac{\pi}{3}\left(1+\varepsilon_a-\frac{1}{R}\sqrt{\frac{N^\alpha D}{2\gamma_{wet}}}\right) \tag{37}$$

and since $\varepsilon_a\ll 1$, the only significant effect of the presence of the liquid is $\gamma_{dry}\to\gamma_{wet}$, namely $a^*_{0wet}\approx a^*_{0dry}(\gamma_{dry}\to\gamma_{wet})$.

A.2. Collapse

The critical pressure in the presence of liquid becomes

$$p_C=\frac{3N^\alpha D}{R^3}-\frac{\gamma_{wet}}{R}-\frac{\gamma_t}{R_B} \tag{38}$$

A.3. Self-collapse

From Eq. (34) we derive the following condition for the self-collapse, i.e. collapse under zero pressure, of a nanotube in a bundle in the absence of liquid ($\gamma_t=p=0$, $\gamma_{wet}\to\gamma_{dry}$):

$$R\geq R^{(N)}_{Cdry}=\sqrt{\frac{2N^\alpha D}{\gamma_{dry}}} \tag{39}$$

In the presence of liquid and without an additional external pressure, the new self-collapse radius can be calculated according to Eq. (34) posing $p=0$ and solving the corresponding third-order polynomial equation. However, a correction with respect to $R^{(N)}_{Cdry}$ can be deduced inserting into Eq. (39) $R=R^{(N)}_{Cdry}(\gamma_{dry}\to\gamma_{wet})(1+\varepsilon_R)$, neglecting the powers of $\varepsilon_R\ll 1$ higher than one and recalling Eq. (34); we accordingly find

$$\varepsilon_R=-\frac{\gamma_t}{2R_B\gamma_{wet}}\sqrt{\frac{3N^\alpha D}{\gamma_{wet}}} \tag{40}$$

Thus, the self-collapse radius in the presence of liquid is

$$R\geq R^{(N)}_{Cwet}=\sqrt{\frac{3N^\alpha D}{\gamma_{wet}}}(1+\varepsilon_R) \tag{41}$$

and since $\varepsilon_R\ll 1$, the only significant effect of the presence of liquid is $\gamma_{dry}\to\gamma_{wet}$, namely $R^{(N)}_{Cwet}\approx R^{(N)}_{Cdry}(\gamma_{dry}\to\gamma_{wet})$.

In contrast, for an isolated nanotube the critical pressure becomes

$$p_C=\frac{3N^\alpha D}{R^3}-\frac{\gamma_t}{R} \tag{42}$$

and thus the role of the liquid is crucial; the self-collapse takes place for

$$R\geq R^{(N)}_C=\sqrt{\frac{3N^\alpha D}{\gamma_t}} \tag{43}$$

Taking $D=0.11$ nN nm (bending stiffness of graphite), $\gamma_t=0.07$ N/m (surface tension of water) we find $2R^{(1)}_C\approx 4.3$ nm. Considering an intermediate coupling between the walls ($\alpha\approx 2$), the critical diameters for double and triple walled nanotubes are $2R^{(2)}_C\approx 8.7$ and $2R^{(3)}_C\approx 13.0$ nm.

Note that for liquids with low surface tension the critical diameter could become quite large, for example for argon $\gamma_t=0.005-0.015$ N/m and $2R^{(1)}_C\approx 9.4-16.2$ nm.

A.4. "Dog-bone" configuration

In the presence of liquid the state equation for the dog-bone configuration becomes

$$p(r)=\frac{N^\alpha D}{2r^3}-\frac{\gamma}{r}-\frac{\gamma_t}{R_B} \tag{44}$$

where $\gamma=\gamma_{in}+\gamma_{out}$ is the total, sum of the inner and outer, surface energy; if the nanotube is not in contact with other surrounding nanotubes $\gamma_{out}=0$; moreover, $\gamma_{in,out}=\gamma_{dry,wet}$ as a consequence of the presence and/or absence inside and/or outside the nanotube of the liquid.

For zero surface energy and tension the equilibrium pressure is positive (inward), whereas complimentary for zero bending stiffness it is negative (outward). Under zero pressure and without liquid ($p=\gamma_t=0$) the equilibrium is reached for

$$r_{0dry}=\sqrt{\frac{N^{\alpha}D}{2\gamma}} \tag{45}$$

In the presence of liquid and without an additional external pressure, the new equilibrium radius can be calculated according to Eq. (44) posing $p=0$ and solving the corresponding third-order polynomial equation. However, a correction with respect to the previously evaluated case of absence of liquid can be deduced inserting into Eq. (44) $r=r_{0dry}(1+\varepsilon_r)$, neglecting the powers of $\varepsilon_r \ll 1$ higher than one and recalling Eq. (45); we accordingly find

$$\varepsilon_r=-\frac{1}{4R_B}\sqrt{\frac{2N^{\alpha}D}{\gamma}} \tag{46}$$

Thus the equilibrium configuration in the presence of liquid is

$$r_{0wet}=\sqrt{\frac{N^{\alpha}D}{2\gamma}}(1+\varepsilon_r) \tag{47}$$

and since $\varepsilon_r \ll 1$, the only significant effect of the presence of the liquid is the modification of γ (in which $\gamma_{dry}\to\gamma_{wet}$).Posing the limiting condition of $r=R/2$ in Eq. (44), we deduce the critical pressure corresponding to the dog-bone "opening" (note that the process is stable, even if rapid around a particular configuration):

$$p_O=\frac{4N^{\alpha}D}{R^3}-\frac{2\gamma}{R}-\frac{\gamma_t}{R_B} \tag{48}$$

Moreover, posing $p_O=0$ in Eq. (48) in absence of liquid ($p_O=\gamma_t=0$) suggests that for nanotube radii:

$$R\le\sqrt{\frac{2N^{\alpha}D}{\gamma}}=2r_{0dry} \tag{49}$$

the "dog-bone" configuration cannot be self-maintained.

In the presence of liquid the new critical radius can be calculated according to Eq. (48) posing $p_O=0$ and solving the corresponding third-order polynomial equation. However, a correction with respect to the previously evaluated case of absence of liquid can be deduced inserting into Eq. (49) $R=2r_{0dry}(1+\varepsilon)$, neglecting the powers of $\varepsilon \ll 1$ higher than one and recalling Eq. (49); we accordingly find

$$\varepsilon=-\frac{\gamma_t}{2R_B\gamma}\sqrt{\frac{N^{\alpha}D}{2\gamma}} \tag{50}$$

Thus the equilibrium configuration in the presence of liquid is

$$R\le\sqrt{\frac{2N^{\alpha}D}{\gamma}}(1+\varepsilon) \tag{51}$$

and since $\varepsilon \ll 1$, the only significant effect of the presence of the liquid is the modification of γ (in which $\gamma_{dry}\to\gamma_{wet}$).

In contrast, for an isolated nanotube, $R_B\to r$ (the liquid pressure acts on the two lobes of radius r) and $\gamma_{out}=0$, thus

$$p(r)=\frac{N^{\alpha}D}{2r^3}-\frac{\gamma_{in}+\gamma_t}{r} \tag{52}$$

Accordingly, all the derived previous equations remain valid with formally $\gamma=\gamma_{in}+\gamma_t$ and $R_B\to\infty$. Thus, the equilibrium is reached for

$$r_0=\sqrt{\frac{N^{\alpha}D}{2\gamma}} \tag{53}$$

and the dog-bone configuration cannot be self-maintained for

$$R\le 2r_0 \tag{54}$$

Appendix B. Collapse pressure and self-collapse of peapods, fullerite crystals and fullerenes

B.1. Peapods

In the case of peapods, the collapse pressure is increased as a consequence of the presence inside the nanotube of the fullerenes; since the critical pressure of fullerenes is much higher than that of a nanotube (see the following), we treat the peapod as a nanotube of finite length L, equal to the (centre–centre) distance between two adjacent fullerenes. Note that the classical buckling formula of cylindrical shells assumes infinite length.

According to elasticity (see Jones, 2006) for a long cylinder the buckling pressure is

$$P_c = \frac{3N^{\alpha}D}{R^3}, \quad L \gg L_c \tag{55}$$

whereas for short cylinders

$$P_c = \frac{4\pi^2 N^{\alpha}D}{RL^2}, \quad L \ll L_c \tag{56}$$

The critical length governing the transition can be calculated equating Eqs. (55) and (56):

$$L_c = \frac{2\pi}{\sqrt{3}}R \tag{57}$$

For intermediate lengths, elasticity poses

$$p_c = \frac{\pi^2\sqrt{\sqrt{1-\nu^2}}N^{\alpha}D}{RL\sqrt{Rt}}, \quad L \sim L_c \tag{58}$$

Comparing Eqs. (55) or (56) with Eq. (58) one would deduce the critical lengths governing the transition, from the short or long to the intermediate lengths.

Moreover, we expect the following pressure generated by the surrounding bundle and/or liquid:

$$p_{\gamma} \approx \frac{\gamma}{R} + \frac{\gamma_t}{R_B} \tag{59}$$

The presence of the liquid around the bundle does not affect significantly the critical pressure, since $R_B \gg R$, whereas for isolated peapod $R_B = R$; accordingly,

$$p_{\gamma} \approx \frac{\gamma + \gamma_t}{R} \tag{60}$$

is valid for both peapods in a bundle (with $\gamma_t = 0$ and γ effective surface energy, thus "wet" in the presence of liquid or "dry" if absent) as well as for an isolated peapod (with $\gamma = 0$). Revisiting the previous elastic results, we thus expect for the buckling of peapods the following regimes:

$$p_C = \frac{3N^{\alpha}D}{R^3} - \frac{\gamma + \gamma_t}{R}, \quad L \gg L_c \tag{61a}$$

$$p_C = \frac{\pi^2\sqrt{\sqrt{1-\nu^2}}N^{\alpha}D}{RL\sqrt{Rt}} - \frac{\gamma + \gamma_t}{R}, \quad L \sim L_c \tag{61b}$$

$$p_C = \frac{4\pi^2 N^{\alpha}D}{RL^2} - \frac{\gamma + \gamma_t}{R}, \quad L \ll L_c \tag{61c}$$

Let us introduce the fullerene content as

$$f = \frac{2R}{L} \tag{62}$$

the previous equation becomes

$$p_C = \frac{3N^{\alpha}D}{R^3} - \frac{\gamma + \gamma_t}{R}, \quad f \ll f_c = \frac{\sqrt{3}}{\pi} \tag{63a}$$

$$p_C = \frac{\pi^2\sqrt{\sqrt{1-\nu^2}}N^{\alpha}D}{2R^2\sqrt{Rt}}f - \frac{\gamma + \gamma_t}{R}, \quad f \sim f_c \tag{63b}$$

$$p_C = \frac{\pi^2 N^{\alpha}D}{R^3}f^2 - \frac{\gamma + \gamma_t}{R}, \quad f \gg f_c \tag{63c}$$

This behaviour is summarized in Fig. 7.

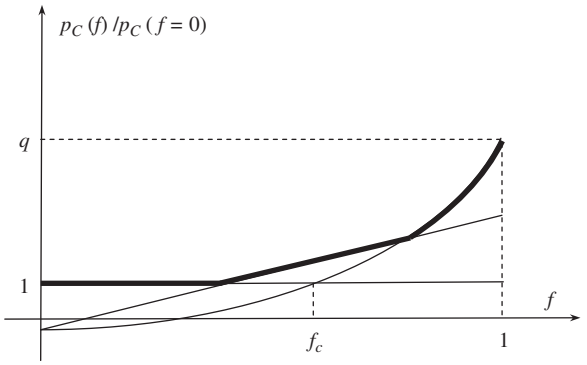

Fig. 7. Theoretical dependence of the nanotube buckling pressure versus fullerene content in a peapod.

We can estimate the ratio q between the buckling pressures for f=0 and 1, as

$$q=\frac{p_C(f=1)}{p_C(f=0)}=\frac{\pi^2-\frac{(\gamma+\gamma_t)R^2}{N^\alpha D}}{3-\frac{(\gamma+\gamma_t)R^2}{N^\alpha D}} \tag{64}$$

Noting that in the treated case $(\gamma+\gamma_t)R^2/(N^\alpha D)\ll 1$, we expect $q\approx\pi^2/3$ (as confirmed by atomistic simulations, J. Elliot, private communication).

From Eqs. (61a)–(61c) we derive the following conditions for the self-collapse, i.e. collapse under zero pressure:

$$R_C^{(N)}=\sqrt{3}\sqrt{N^\alpha}\sqrt{\frac{D}{\gamma+\gamma_t}},\quad L\gg L_c \tag{65a}$$

$$R_C^{(N)}L_C^{(N)2}=\frac{\pi^4D^2\sqrt{1-\nu^2}}{(\gamma+\gamma_t)^2t},\quad L\sim L_c \tag{65b}$$

$$L_C^{(N)}=\sqrt{2\pi}\sqrt{N^\alpha}\sqrt{\frac{D}{\gamma+\gamma_t}},\quad L\ll L_c \tag{65c}$$

Note that for small fullerene content the self-collapse is dictated by a critical radius, as for empty nanotubes, whereas for large fullerene content the self-collapse is dictated by a critical distance between two adjacent fullerenes (in the intermediate case, length and radius are comparable).

B.2. Fullerite crystals and fullerenes

Similarly, the critical pressure of fullerenes in a fullerite crystal is

$$p_C=\frac{2}{\sqrt{3(1-\nu^2)}}\frac{N^\alpha Et^2}{R^2}-\frac{2\gamma}{R}-\frac{2\gamma_t}{R_B} \tag{66}$$

where $1\le\alpha\le 2$ described the interaction between the walls; the first term is that posed by elasticity (that considers α=2; see for instance Pogorevol, 1988), whereas the factor of two in the surface energy and tension is expected according to Laplace's equation.

The presence of the liquid around the crystal does not affect significantly the critical pressure, since $R_B\gg R$, whereas for isolated fullerene R_B=R; accordingly,

$$p_C=\frac{2}{\sqrt{3(1-\nu^2)}}\frac{N^\alpha Et^2}{R^2}-\frac{2(\gamma+\gamma_t)}{R} \tag{67}$$

is valid for both fullerenes in fullerite (with γ_t=0 and γ effective surface energy, thus "wet" in the presence of liquid or "dry" if absent) as well as for an isolated fullerene (with γ=0).

Note that the factor $(t/R)^2$ for fullerenes, appearing instead of $(t/R)^3$ for nanotubes, shows that the critical pressure for fullerenes is much higher than that for nanotubes, at least for $t/R\ll 1$.

From Eq. (67) we derive the following condition for the self-collapse, i.e. collapse under zero pressure of fullerenes in crystals or isolated:

$$R_C^{(N)}=\frac{N^\alpha Et^2}{\sqrt{3(1-\nu^2)}(\gamma+\gamma_t)} \tag{68}$$

Note that for $\nu=0$, $N=1$, $E=1$ T Pa, $t=0.34$ nm, $2(\gamma+\gamma_t)=0.4$ N/m, we find $R_C^{(1)}\approx 334$ nm, showing that fullerenes are highly stable and thus that peapods with high fullerene concentrations are ideal solution against nanotube buckling.

References

Baughman, R.H., Cui, C., Zakhidov, A.A., Iqbal, Z., Barisci, J.N., Spinks, G.M., Wallace, G.G., Mazzoldi, A., Rossi, D.D., Rinzler, A.G., Jaschinski, O., Roth, S., Kertesz, M., 1999. Carbon nanotube actuators. Science 284, 1340–1344.

Berger, C., Song, Z., Li, X., Wu, X., Brown, N., Naud, C., Mayou, D., Li, T., Hass, J., Marchenkov, A.N., Conrad, E.H., First, P.N., de Heer, W.A., 2006. Electronic confinement and coherence in patterned epitaxial graphene. Science 312, 1191–1196.

Dalton, A.B., Collins, S., Munoz, E., Razal, J.M., Ebron, Von H., Ferraris, J.P., Coleman, J.N., Kim, B.G., Baughman, R.H., 2003. Super-tough carbon-nanotube fibres. Nature 423, 703.

Dikin, D.A., Stankovich, S., Zimney, E.J., Piner, R.D., Dommett, G.H.B., Evmenenko, G., Nguyen, S.T., Ruoff, R.S., 2007. Preparation and characterization of graphene oxide paper. Nature 448, 457–460.

Elliott, J.A., Sandler, J.K., Windle, A.H., Young, R.J., Shaffer, M.S., 2004. Collapse of single-wall carbon nanotubes is diameter dependent. Physical Review Letters 92, 095501.

Endo, M., Muramatsu, H., Hayashi, T., Kim, Y.A., Terrones, M., Dresselhaus, M.S., 2005. Nanotechnology: 'Buckypaper' from coaxial nanotubes. Nature 433, 476.

Ericson, L.M., Fan, H., Peng, H., Davis, V.A., Zhou, W., Sulpizio, J., Wang, Y., Booker, R., Vavro, J., Guthy, C., Parra-Vasquez, A.N.G., Kim, M.J., Ramesh, S., Saini, R.K., Kittrell, C., Lavin, G., Schmidt, H., Adams, W.W., Billups, W.E., Pasquali, M., Hwang, W.-F., Hauge, R.H., Fischer, J.E., Smalley, R.E., 2004. Macroscopic, neat, single-walled carbon nanotube fibers. Science 305, 1447–1450.

Jiang, K., Li, Q., Fan, S., 2002. Nanotechnology: spinning continuous carbon nanotube. Nature 419, 801.

Koziol, K., Vilatela, J., Moisala, A., Motta, M., Cunniff, P., Sennett, M., Windle, A., 2007. High-performance carbon nanotube fiber. Science 318, 1892–1895.

Li, Y.-L., Kinloch, I.A., Windle, A.H., 2004. Direct spinning of carbon nanotube fibers from chemical vapor deposition synthesis. Science 304, 276–278.

Motta, M.S., Moisala, A., Kinloch, I.A., Windle, A.H., 2007. High performance fibres from 'Dog Bone' carbon nanotubes. Advanced Materials 19, 3721–3726.

Novoselov, K.S., Geim, A.K., Morozov, S.V., Jiang, D., Zhang, Y., Dubonos, S.V., Grigorieva, I.V., Firsov, A.A., 2004. Electric field effect in atomically thin carbon films. Science 306, 666–669.

Pogorevol, A.V., 1988. Bending of Surface and Stability of Shells, American Mathematical Society, Providence, Rhode Island, USA.

Pugno, N., 2006. New quantized failure criteria: application to nanotubes and nanowires. International Journal of Fracture 141, 311–323.

Pugno, N., 2006. Dynamic quantized fracture mechanics. International Journal of Fracture 140, 159–168.

Pugno, N., 2006. Mimicking nacre with super-nanotubes for producing optimized super-composites. Nanotechnology 17, 5480–5484.

Pugno, N., 2007. Young's modulus reduction of defective nanotubes. Applied Physics Letters 90, 043106–0431/3.

Pugno, N., 2008. An analogy between the adhesion of liquid drops and single walled nanotubes. Scripta Materialia 58, 73–75.

Pugno, N., Ruoff, R., 2004. Quantized fracture mechanics. Philosophical Magazine 84/27, 2829–2845.

Pugno, N.M., 1999. Optimizing a non-tubular adhesive bonded joint for uniform torsional strength. International Journal of Materials and Product Technology 14, 476–487.

Pugno, N.M., 2006. On the strength of the nanotube-based space elevator cable: from nanomechanics to megamechanics. Journal of Physics: Condensed Matter 18, S1971–S1990.

Pugno, N.M., 2007. Nano-friction, stick-slip and pull-out forces in nanotube-multiwalls, -composites and -bundles. Journal of the Mechanical Behavior of Materials 18 (4), 265–281.

Pugno, N.M., 2007. Space elevator: out of order? Nano Today 2, 44–47

Pugno, N.M., 2009. Analytical modeling of the self-collapse and sliding failure of nanotubes in a bundle: implications for a flaw tolerant design of the space elevator cable. In: Third International Conference on Space Elevator, Cnt Tether Design, and Lunar Industrialization Challenges, December 5–6, Luxembourg, Luxembourg (Invited Top Speaker Lecture).

Pugno, N.M., Carpinteri, A., 2003. Tubular adhesive joints under axial load. Journal of Applied Mechanics 70, 832–839.

Pugno, N.M., Cornetti, P., Carpinteri, A., 2008. On the impossibility of separating nanotubes in a bundle by a longitudinal tension. Journal of Adhesion 84, 439–444.

Pugno, N.M., 2007. The role of defects in the design of the space elevator cable: from nanotube to megatube. Acta Materialia 55, 5269–5279.

Jones, R.M., 2006. Buckling of bars, plates and shells, Bull Ridge Publishing, Blacksburg, Virginia, USA.

Stankovich, S., Dikin, D.A., Dommett, G.H.B., Kohlhaas, K.M., Zimney, E.J., Stach, E.A., Piner, R.D., Nguyen, S.T., Ruoff, R.S., 2006. Graphene-based composite materials. Nature 442, 282–285.

Wang, S., Liang, Z., Wang, B., Zhang, C., 2007. High-strength and multifunctional macroscopic fabric of single-walled carbon nanotubes. Advanced Materials 19, 1257–1261.

Wu, Z., Chen, Z., Du, X., Logan, J.M., Sippel, J., Nikolou, M., Kamaras, K., Reynolds, J.R., Tanner, D.B., Hebard, A.F., Rinzler, A.G., 2004. Transparent conductive carbon nanotube films. Science 305, 1276.

Zhang, M., Atkinson, K.R., Baughman, R.H., 2004. Multifunctional carbon nanotube yarns by downsizing an ancient technology. Science 306, 1358–1361.

Zhang, M., Fang, S., Zakhidov, A.A., Lee, S.B., Aliev, A.E., Williams, C.D., Atkinson, K.R., Baughman, R.H., 2005. Strong, transparent, multifunctional, carbon nanotube sheets. Science 309, 1215–1219.

Zhu, H.W., Xu, C.L., Wu, D.H., Wei, B.Q., Vajtai, R., Ajayan, P.M., 2002. Direct synthesis of long single-walled carbon nanotube strands. Science 296, 884–886.